

1 International airport emissions and their impact on local air 2 quality: Chemical speciation of ambient aerosols at Madrid- 3 Barajas Airport during AVIATOR Campaign

4 Saleh Alzahrani¹, Doğuşan Kılıç^{1,2}, Michael Flynn¹, Paul I. Williams^{1,2} and James Allan^{1,2}

7 ¹Department of Earth and Environmental Sciences, University of Manchester, Manchester, UK

8 ²National Centre for Atmospheric Science, University of Manchester, Manchester, UK

10 *Correspondence to:* Saleh Alzahrani (Saleh.alzahrani@manchester.ac.uk)

14 **Abstract.** Madrid-Barajas International Airport (MAD), located in Spanish Capital Madrid, is the fourth-busiest
15 airport in Europe. As part of the AVIATOR campaign, chemical composition of particulate matter and other key
16 pollutants were measured at the airport perimeter during October 2021, to assess the impact of airport emissions
17 on local air quality. A high-fidelity ambient instrumentation system was deployed at Madrid Airport to measure:
18 composition of ambient aerosol and concentrations of black carbon (*e*BC), carbon dioxide (CO₂), carbon monoxide
19 (CO), nitrogen dioxide (NO_x), sulphur dioxide (SO₂), particulate matter (PM_{2.5}, PM₁₀), total hydrocarbon (THC),
20 and total particle number. The average concentration for the entire campaign of *e*BC, NO_x, SO₂, PM_{2.5}, PM₁₀, CO
21 and THC at the airport were, 1.07 (µg/m³), 22.7 (µg/m³), 4.10 (µg/m³), 9.35 (µg/m³), 16.43 (µg/m³), 0.23 (mg/m³)
22 and 2.30 (mg/m³) respectively. The source apportionment analysis of the non-refractory organic aerosol (OA)
23 using positive matrix factorisation (PMF) allowed us to discriminate between different sources of pollution,
24 namely: Less Oxidised Oxygenated Organic Aerosol (LO-OOA), Alkane Organic Aerosol (AlkOA), and More
25 Oxidised Oxygenated Organic Aerosol (MO-OOA) source. The results showed that LO-OOA and MO-OOA
26 accounts for more than 80% of the total organic particle mass that was measured near runway at the airport. Trace
27 gases correlate better with AlkOA factor more than LO-OOA and MO-OOA which indicate that AlkOA is mainly
28 related to the primary emissions of combustion. Bivariate polar plots were used for the source identification.
29 Significantly higher concentrations of the obtained factors were observed at low wind speeds < 3m/s from the
30 southwest where two of runways, as well as all terminals are located. Higher SO₂/NO_x and CO/*e*BC ratios were
31 observed when the winds originating from the northeast where the 18L/36R runways are located. This is attributed
32 to the aircraft influence and the lack of a local road source in the northeast area.

35 1. Introduction

37 Several studies have linked particulate matter (PM) to a range of harmful health effects, including respiratory and
38 cardiovascular ailments (Boldo et al., 2006; Li et al., 2003a; Pope and Dockery, 2006; Schwarze et al. et al., 2006).
39 In recent years, a number of researchers have found an association between aviation emissions and potential
40 adverse human health impacts. These emissions can lead to immune system malfunction, various pathologies, the
41 development of cancer, and premature death. Hence, it is increasingly recognised as a serious, worldwide public
42 health concern (Yim et al., 2013; He et al., 2018; Jonsdottir et al., 2019).
43 A few studies have reported that air pollutants emitted from large airports can play a vital role in worsening the
44 regional air quality (Rissman et al., 2013; Hudda and Fruin, 2016). Hu et al., (2009) and Westerdahl et al., (2008)
45 measured high ambient PM concentrations downwind of Los Angeles International Airport (LAX) and Santa
46 Monica Airport (SMA) in California. A decline in the ambient air quality was observed over distances of up to
47 18 km downwind from international airports owing to gas turbine-emitted PM (Hudda et al., 2014; Hudda and
48 Fruin, 2016). Airports' contribution to primary and secondary inhalable and fine particulate matter (PM₁₀ and
49 PM_{2.5}, mass of particles with aerodynamic diameters <10 µm and <2.5 µm, respectively) making them
50 determinants of the air quality in cities and a significant issue for the local air quality management. To date, several
51 questions still remain to be answered regarding the chemical composition of aircraft plumes, and the health risks
52 associated with the exposure to the pollutants originating from airports in neighbouring communities. Responding
53 to the growing concern about the risk of exposure to airport pollutants, studies have been conducted to gain a
54 better understanding of airport emissions and their possible effects on local and regional air quality. Thus far,
55 aircraft engines are considered to be one of the major sources of both gaseous and particulate pollutants at the
56 airport (Masiol and Harrison, 2014). Various campaigns have reported both physical and chemical properties of
57 particulate and gaseous emissions (Kinsey, 2009; Kinsey et al., 2010, 2011; Mazaheri et al., 2011; Hudda et al.,

58 2016). Aviation fuel Jet A1 is the most common type of fuel that is used in civil aviation. It's a complex mixture
59 of aliphatic hydrocarbons and aromatic compounds, characterized by a mean C/H ratio of ~ 0.52 (with an average
60 empirical molecular formula of C₁₂H₂₃) (Lee et al., 2010). The paraffins fractions in jet fuel typically make up
61 over 75% of the fuel by weight, while the aromatic content is less than or equal to 25% (Liu et al., 2013). Several
62 fuel combustion sources are present at airports, including aircraft operation and diesel ground transport that
63 services the airport and brings in passengers for traveling. Fuel combustion likely caused maximum particle counts
64 in 10 - 20 nm range based on the particle size distribution analysis (Zhu et al., 2011). There are also other sources
65 of airport-related PM emissions that contribute to air pollution at the local scale. Particulate pollution (38% of
66 PM10 with a mean level of 48 µg/m³) at airports can periodically originate from the construction activities for
67 terminal maintenance and construction (Amato et al., 2010). Particles emitted by commercial aircraft can be
68 divided into two main groups: non-volatile and volatile PM. Non-volatile PM (nvPM) is usually formed during
69 the (incomplete) combustion process and then emitted from the aircraft combustion chamber. It consists mostly
70 of carbonaceous substances such as soot, dust, and trace metals (Yu et al., 2019). nvPM has the physical property
71 of being resistant to high temperatures and pressure. On the other hand, volatile PM is formed through gas to
72 particle conversion process, primarily by sulphur and organic compounds, which exist in the exhaust gas
73 downstream of the engine after emission. Sulphuric compounds are formed as a result of sulphur in fuel, whereas
74 organic particles are formed as combustion products, and from fuel and oil vapours (ICAO, 2016; Smith et al.,
75 2022). Aircraft and ground unit emissions have been documented in prior research (Masiol and Harrison, 2014),
76 yet there is still a gap in knowledge about airport-related PM emissions in terms of (i) apportioning PM to
77 individual sources at airports, (ii) specifying their chemical composition, and (iii) the wider impacts of PM on
78 local communities. This study set out to obtain data that will help to address these research gaps by providing
79 further in-depth information on particle composition measurements and key pollutants observed within an airport
80 environment, through characterizing organic volatile PM emissions aiming to assess the effect of aviation
81 emissions on the local air quality. Here we focus on Adolfo Suárez Madrid-Barajas Airport in Madrid. As part of
82 the AVIATOR Project (Assessing aViation emission Impact on local Air quality at airports: TOwards Regulation),
83 several experiments were conducted at the Madrid-Barajas Airport, for monitoring the chemical properties of
84 sub-micron particles. Source apportionment analysis was performed based on the particle data collected via high
85 resolution mass spectrometry and this analysis allowed us to discriminate between different sources of pollution
86 at the airport microenvironment. These findings will serve as the foundation for additional comprehensive
87 research, such as toxicological and health effect studies of PM originating from aviation activities.
88

89 2. Methods

90 2.1. Description of the sampling location

92 Adolfo Suárez Madrid-Barajas Airport is the main international airport in Spain, located within the municipal
93 limits of Madrid, 13 km northeast of Madrid's city centre. It is the fourth-busiest airport in Europe based on
94 passenger volume (Eurostat Database, 2021). In 2019, 62 million travellers used Madrid-Barajas and nearly half
95 a million aircraft movements have been recorded, making it the largest and busiest airport in the country. In 2021,
96 nearly one-third of the previous number travelled through Madrid Airport because of the COVID-19 pandemic.
97 The airport has five passenger terminals named T1, T2, T3, T4, and T4S. Barajas Airport has four runways: two
98 on the north-south axis and parallel to each other 18L/36R - 18R/36L and two on the northwest-southeast axis
99 14L/32R - 14R/32L. The runways enable takeoff and landing simultaneously at the airport, allowing 120
100 operations per hour (one takeoff or landing every 30 seconds). The sampling location was chosen in concert with
101 AENA, the owner and operator of the Barajas Airport to facilitate the provision of power and access for servicing.
102 Focusing on the temporal and spatial monitoring of the key pollutants, the site was positioned between runways
103 36L and 36R to sample the airport emissions from an optimal sampling point for aviation activities (Fig.1). The
104 distance from sampling location to the runways 18L/36R, 18R/36L, 14L/32R and 14R/32L are 680 m, 620 m, 3.2
105 km, and 4.1 km respectively. Furthermore, the distance between sampling location and adjacent terminals T1, T2,
106 T3 is approximately 5 km whereas 3 km and 1.5 km to the terminals T4 and TS4 respectively. The nearest highway
107 is located around 2.6 km away from the sampling location.
108

Formatted: Underline, Highlight

Formatted: Underline, Highlight

Formatted: Underline, Highlight

Formatted: Underline, Highlight

Formatted: Underline, Highlight

Formatted: Underline, Highlight

Formatted: Underline

Formatted: Underline, Highlight

Formatted: Underline

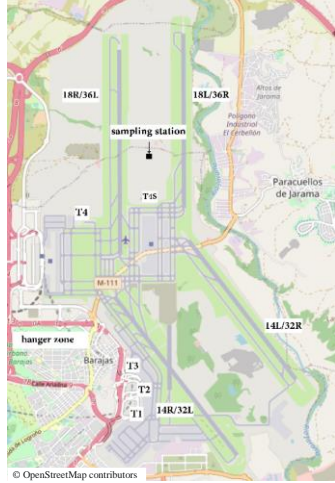


Figure 1. Locations of runways, terminals, and sampling site at Adolfo Suárez Madrid-Barajas Airport. Measurements were performed between October 8, 2021 and October 23, 2021. (Adapted from: <https://www.openstreetmap.org>)

2.2. Sampling and instrumentation

The autumn campaign of AVIATOR took place in October 2021. Sampling was conducted continuously, starting at 12:00 pm on October 8, 2021 and ending at 20:00 pm on October 23, 2021. An ambient instrumentation system with specific reference to PM was deployed at Madrid Airport to better characterise air quality at the airport microenvironment. The measurement equipment of the system includes an Aerodyne High-Resolution Time-of-Flight Aerosol Mass Spectrometer (AMS) for the chemical speciation of the particles. AMS measures concentration and chemical composition of non-refractory aerosols online. AMS provided high-resolution measurements of primary and secondary organic aerosol and inorganic aerosol including sulphates, nitrates, and ammonium, from approximately 60 nm to 600 nm with 100 % transmission, extending to smaller and larger sizes with reduced transmission (Canagaratna et al., 2007). An aerodynamic lens is used to draw aerosols into a vacuum chamber. Particles are focused into a narrow beam and accelerated to a velocity inversely related to their vacuum aerodynamic diameter. The particles impact on a tungsten surface, heated to 600 °C, which causes them to flash vaporise. A 70-eV electron is used to ionize the vapours before they are analysed by mass spectrometry. During the measurement period, AMS was sampling with 1µm cut-off inlet and at 30 s time resolution. In addition to standard AMS flow, baseline and single ion calibrations every second day, an ammonium nitrate solution was atomised to calibrate the AMS (for size-dependent ionisation efficiency). The analysis of the chemical characteristics of aircraft PM using an AMS have been described elsewhere in detail (Yu et al., 2010; Anderson et al., 2011; Smith et al., 2022). Equivalent black carbon mass concentration (*e*BC) based on aerosol optical absorption was monitored using the Multi-Angle Absorption Photometer (MAAP) during this campaign. The MAAP operates at 670nm wavelength, has a 10s-time response with a flow rate of 8 litre/min, for unattended long-term monitoring of carbonaceous particulate emissions from combustion sources (Petzold and Schonlinner, 2004). MAAP has been used for the monitoring of black carbon emission from aviation (Herndon et al., 2008; Timko et al., 2014). The instrument was set up to measure average *e*BC concentrations with one-minute intervals. By using a condensation particle counter (CPC), TSI model 3750 ($D_{50} \approx 7\text{nm}$), total particle number concentration was measured real-time to capture temporal variability in particle number concentrations with a measurement range of up to 100,000 particles/cm³ and a time resolution of one second. Ambient CO₂ concentration near runways were also measured by a LI-COR CO₂ Trace Gas Analysers at 1-sec intervals. In addition, meteorological parameters (temperature, pressure, relative humidity, wind speed, and direction) were measured at the site with the instrumentation system. The system was co-located with AENA (REDAIR) fixed monitoring site to provide additional spatially resolved data. The REDAIR station monitors the concentration of sulphur dioxide (SO₂), nitrogen dioxide (NO_x), carbon monoxide (CO), ozone (O₃), suspended particles PM (including PM_{2.5}, PM₁₀), and total hydrocarbon (THC) with a time resolution of 30 minutes.

Formatted: Underline, Highlight

Formatted: Underline, Highlight

149
150
151
152
153
154
155
156
157
158
159
160
161
162
163
164
165
166
167
168
169
170
171
172
173
174
175
176
177
178
179
180
181
182
183
184
185
186
187

2.3. Data analysis

AMS was operating in Mass Spectrum (MS) mode to identify the chemical species present in the aerosol ensemble and quantify the overall mass loading. AMS data were analysed using the data analysis toolkit TOF-AMS SQUIRREL v1.65B, operated within Igor Pro (WaveMetrics, Inc.). The Source Finder (SoFi) is a software package designed to analyse multivariate data using state-of-the-art source apportionment techniques to understand the sources of various pollutants (Canonaco et al., 2013). SoFi, running under IGOR 6.37, was used to deconvolve organic aerosol emissions via the Positive Matrix Factorization (PMF) model. The PMF model, implemented through the multiline engine version 2 (ME-2) factorisation tool, was used to determine the number of factors (sources). ME-2, a multivariate solver, employs the same mathematical/statistical method as PMF to evaluate solutions (Paatero, 1999). ME-2 equations are designed for analysing and calculating the relative contributions of various source pollutants by measuring their concentration at receptor locations (Paatero and Tapper, 1994). The PMF model processes many variables and categorises them into two types (i) source types, which can be determined based on the chemical composition of the pollutants, and (ii) source contributions, used to quantify the amount of contribution from each source to a sample. PMF inputs were restricted to only non-negative concentrations since no sample can have a negative source contribution. A step-by-step approach was employed to select the number of solutions (factors). The method described by Reyes et al. (2016) and Smith et al. (2022) was followed to determine the optimal solution. This approach began initially with a two-factor model and then incrementally increased to a maximum of five factors. PMF analysis was performed with seed runs and varying FPEAK values (ranging from -1 to 1 with steps of 0.1) to better differentiate organic aerosol sources. Seed runs and FPEAK are rotational techniques in the ME-2 tool, and they represent one of the unconstrained PMF run approaches used for the exploration of the solution space. During the analysis, it was noted that factor four consistently correlates with factor five, exhibiting identical time series and similarities in mass spectra. This difficulty in separation has previously been observed in the case of well-mixed pollutants, attributed to low temperatures and wind speeds (Reyes et al., 2018). Greater stability was achieved when analysing 3-factor solutions with varying FPEAK values. During the analysis, seed runs and PMF with FPEAK solutions showed no significant variation in the normalised scaled residuals parameter (Q / Qexp), with values close to 1. This is reasonable given that PMF determines the solution by minimising this value (Reyes et al., 2016). The factorisation strategy was entirely successful in separating three different sources, each with distinct mass spectra and differing time series. Consequently, 3-factor solutions emerged as the optimal number of sources, demonstrating the best performance with the lowest residuals and Q/Qexp values close to 1. Furthermore, the obtained solution exhibited the most favorable results, characterized by distinct diurnal trends and dissimilarities in time series and mass-to-charge ratios among the factors.

3. Results and Discussion

3.1 Variations of organic, inorganic, and oil emissions

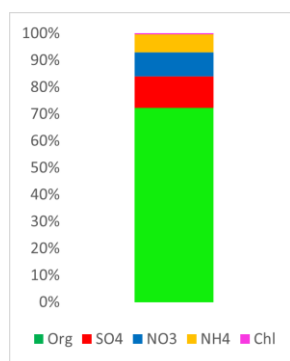


Figure 2. The bar chart shows aerosol fractions where organic and sulphate species account for more than 80% of the total aerosol mass.

Mass concentrations of organic and inorganic aerosols was $9.6 \mu\text{g}/\text{m}^3$ on average for the entire campaign. Organic aerosols, with a significantly high fraction compared to the nearest sulphate with 15 % accounts for about 70% of the total aerosols measured by AMS. Figure 2 shows aerosol fractions where organics account for about 70% of

Formatted: Underline, Highlight

Formatted: Underline, Highlight

Formatted: Underline, Highlight

Formatted: Underline, Highlight

Formatted: Underline, Highlight

Formatted: Underline, Highlight

Formatted: Underline, Highlight

Formatted: Underline, Highlight

Formatted: Underline, Highlight

Formatted: Underline, Highlight

Formatted: Underline, Highlight

Formatted: Underline, Highlight

Formatted: Underline, Highlight

Formatted: Underline, Highlight

Formatted: Underline, Highlight

Formatted: Underline, Highlight

Formatted: Underline, Highlight

Formatted: Underline, Highlight

Formatted: Underline, Highlight

Formatted: Underline, Highlight

Formatted: Underline, Highlight

Formatted: Underline, Highlight

Formatted: Underline, Highlight

Formatted: Underline, Highlight

Formatted: Underline, Highlight

Formatted: Underline, Highlight

Formatted: Underline, Highlight

Formatted: Underline, Highlight

Formatted: Underline, Highlight

Formatted: Underline, Highlight

Formatted: Underline, Highlight

Formatted: Underline, Highlight

Formatted: Underline, Highlight

Formatted: Underline, Highlight

Formatted: Underline, Highlight

Formatted: Underline, Highlight

Formatted: Underline, Highlight

Formatted: Underline, Highlight

Formatted: Underline, Highlight

Formatted: Underline, Highlight

Formatted: Underline, Highlight

Formatted: Underline, Highlight

Formatted: Underline, Highlight

Formatted: Underline, Highlight

Formatted: Underline, Highlight

Formatted: Underline, Highlight

Formatted: Underline, Highlight

Formatted: Underline, Highlight

188
189
190
191
192
193
194
195

196 the aerosol. The PMF analysis in this paper mainly focuses on the composition of the organic mass concentration.
 197 Pprevious studies have shown that lubrication oil has been detected in ambient air near runways, and it may further
 198 add to the total organic PM emissions due to aircraft engine operations (Timko et al., 2010b; Yu et al., 2010;
 199 Fushimi et al., 2019; Ungeheuer et al., 2022). Aircraft plume measurements indicated that oil was found to
 200 contribute 5% to 100% (Yu et al., 2012). The m/z 85 signal is a well-known oil signal in the AMS mass spectrum.
 201 Ratio of m/z 85:71 is used as a marker for oil (Fig. 3). The ratio of 0.66 was used as a benchmark for oil
 202 contribution (Yu et al., 2012). A value less than 0.66 can be considered oil-free organic PM and conversely, any
 203 value larger than 0.66 indicates the presence of lubrication oil. However, based on the AMS measurements during
 204 AVIATOR autumn campaign, lubrication oil accounted only up to 5% of the total aerosol mass, which is
 205 significantly less compared to the measurements of Yu et al. (2012). There are three probable explanations on the
 206 deficiency of AMS to detect oil precursors: (i) the oil particles are too small in diameter for AMS to detect, (ii)
 207 complete pyrolysis of the oil in the engine combustion zone forming carbon monoxide (CO) and carbon dioxide
 208 (CO₂) (Smith et al., 2022) or (iii) oil particles contribute to an insignificant amount (by mass) of organic mass in
 209 engine exhaust therefore are not detected. Additional factors that could potentially impact the minimal presence
 210 of oil lubrication in this analysis might involve the overall mass loading of aerosols, the influence of urban aerosol
 211 emissions, or the proximity of the sampling point to the nearest runways. Additional information on how the
 212 lubrication oil ratio, as measured by AMS, varies with wind speed and direction, is provided in the supplementary
 213 material (Fig.S4). During the AVIATOR autumn campaign, measuring oil was challenging due to the prevalent
 214 urban background. A "little oil" region was identified at low to moderate wind speeds (2–5 m/s) originating from
 215 the southwest, encompassing terminal buildings (T1, T2, T3, T4, and TS4), two runways (14R/32L and 18R/36L),
 216 and a hangar zone. In contrast, a region "unlikely to contain oil" was noted when winds came from the northeast
 217 of the airport, near runways 18L/36R, with relatively higher wind speeds (above 5 m/s). Furthermore, Fig.S5
 218 displays the daily lubrication oil ratio throughout the sampling period, pinpointing Sunday, October 16th, as the
 219 only day when the lubrication oil ratio surpassed 0.66. On other days, the ratio suggested a minimal likelihood of
 220 oil presence. An hourly analysis within Fig.S5 reveals that the lubrication oil ratio exceeded 0.66 only at 20:00,
 221 aligning with the evening peak in PM_{2.5} concentrations Fig.S3. This suggests a significant influence of urban
 222 background aerosols on the lubrication oil measurements. Since PMF analysis is based on the organic masses
 223 measured via AMS, lubrication oil is not identified as a determinant and there is no oil organic mass profile
 224 reported in previous studies and here (Ulbrich et al., 2009). PMF has been proven inefficient at detecting such
 225 levels (Ulbrich et al., 2009), therefore, oil contribution to the organic mass may be under-represented in this study.

Formatted: Underline, Highlight

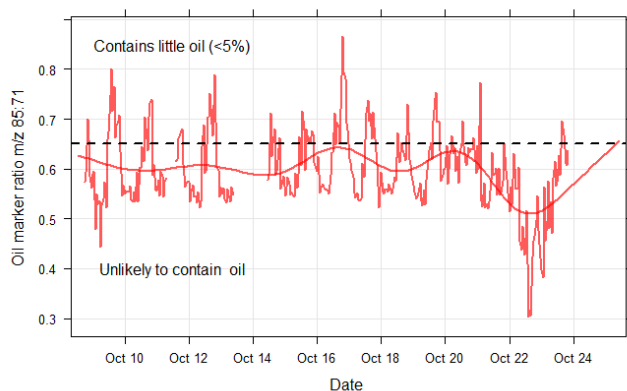
Formatted: Underline, Highlight

Formatted: Underline, Highlight

Formatted: Underline, Highlight

Formatted: Underline, Highlight

Formatted: Underline, Highlight



226 **Figure 3. Temporal variability of lubrication oil fraction in total aerosol mass obtained from AMS measurements.**
 227 **The ratio of m/z 85/71 was used as the mass marker to identify lubrication oil. The analysis showed that no oil or very**
 228 **little (<5%) oil fraction was detected.**

229 **3.2 PMF Analysis**
 230
 231

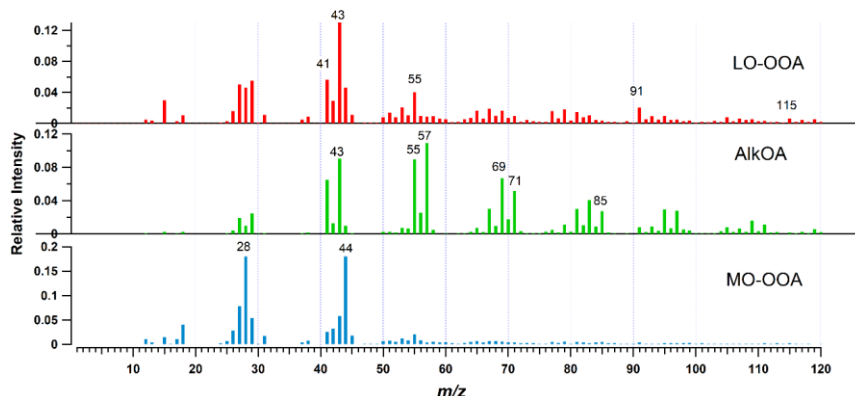


Figure 4. The mass spectral fingerprint of the three factors from the PMF solutions. Less Oxidised Oxygenated Organic Aerosol (LO-OOA), Alkane Organic Aerosol (AlkOA), and More Oxidised Oxygenated Organic Aerosol (MO-OOA), which can be indicative of secondary aerosols. Selected mass markers with a relative intensity higher than 0.01 are numbered.

The PMF analysis in this study aims to provide relative contribution of the sources of aerosols near runway. In addition to determining the diurnal pattern of the obtained factors during the autumn campaign, PMF solutions were used to investigate how meteorology affects airborne particulate pollution. During AVIATOR autumn campaign at Madrid-Barajas International Airport three sources were identified via PMF (Fig. 4 shows the results of the PMF analysis, the mass spectral fingerprint). The first factor in Fig. 4, LO-OOA, stands for Less Oxidised Oxygenated Organic Aerosol. It is a type of secondary organic aerosol (SOA) characterized by its low degree of oxidation. LO-OOA are formed in the atmosphere through the oxidation of volatile organic compounds (VOCs), which can originate from a variety of anthropogenic sources. In this analysis LO-OOA shows the presence of an aromatic marker at m/z 115, a marker used for identifying indene (C_9H_8) ion in previous studies focusing on aviation emissions (Timko et al., 2014; Smith et al., 2022). LO-OOA is associated with aromatic fragments at m/z 77, 91, 105, 115 and presents a high relative intensity (0.13) at m/z 43 (characteristic of LO-OOA) and a lower relative intensity (<0.04) at m/z 91 which is related to toluene ion (C_7H_7) (Smith et al., 2022). Ambient temperature plays a crucial role in influencing the LO-OOA factor, displaying significant diurnal fluctuations. The lowest concentrations of LO-OOA are recorded at midday, coinciding with the peak in ambient temperatures (Fig. 5). A prior PMF analysis of organic particulate matter from aircraft emissions revealed a significant aromatic factor within the organic PM, characterized by elevated signals at m/z 77, 91, 105, 115, 128 (Timko et al., 2014). The aromatic factor identified by Timko et al. (2014) was found to dominate the organic PM emissions from turbojet engines at low-thrust settings. It was associated with the products of incomplete combustion and exhibited high variability, which varied with engine power settings (the sum of signals in the factor decreased as engine power increased). Another study by Smith et al. (2022), investigated the chemical composition of organic aerosols emitted by gas turbines and identified a Semi-Volatile Oxygenated Organic Aerosol (SV-OOA) factor, which forms through oxidative processes near the engine exit. A strong correlation ($R = 0.91$) and similarity in mass spectra between the LO-OOA in this study and the SV-OOA described by Smith et al. (2022) were observed. Owing to the absence of volatility measurements during this period and the limited time for aging (no more than a few minutes), we consider the LO-OOA factor in our analysis to be the most accurate estimate available, rather than the SV-OOA as suggested by Smith et al. (2022). The second factor, identified based on the PMF analysis of Madrid airport sample, is Alkane Organic Aerosol (AlkOA) factor. It is associated with unburned fuel and emissions from incomplete combustion, exhibiting high relative intensities at m/z 43, 57, and 85, indicative of decane ($C_{10}H_{22}$), a common alkane in jet fuel. Given that mass spectral fingerprint of decane is similar to the other aliphatic hydrocarbons (e.g., long-chain alkanes) found in Jet A1 fuel, as reported by Yu et al. (2012) and Smith et al. (2022). AlkOA factor referred here as a marker to identify emissions originating from unburnt fuel/incomplete fuel combustion products. Previously, primary aliphatic factor was found in PMF analysis by Timko et al. (2014) and was characterized by increased signals at masses such as 41/43, 55/57, 69/71, 83/85. Each of these masses correspond to an alkane. The primary aliphatic factor in Timko et al. (2014) study was strongly correlated with black carbon soot emissions under high-power conditions. The strong association between the primary aliphatic factor and soot emissions suggests they originate from similar combustion processes. Timko et al. (2014) concluded that the primary aliphatic factor is derived from combustion related sources and can potentially contain

Formatted: Underline, Highlight

Formatted: Underline, Highlight

Formatted: Underline, Highlight

Formatted: Underline, Highlight

Formatted: Underline, Highlight

Formatted: Underline, Highlight

Formatted: Underline, Highlight

Formatted: Underline, Highlight

Formatted: Underline, Highlight

Formatted: Underline, Highlight

Formatted: Underline, Highlight

Formatted: Underline, Highlight

Formatted: Underline, Highlight

Formatted: Underline, Highlight

Formatted: Underline, Highlight

Formatted: Underline, Highlight

Formatted: Underline, Highlight

Formatted: Underline, Highlight

Formatted: Underline, Highlight

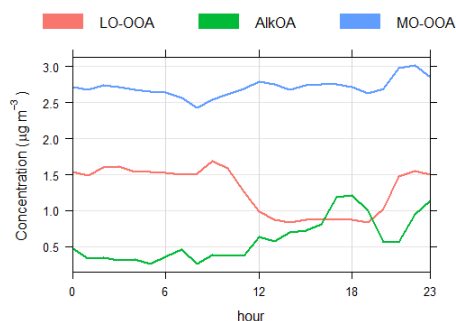
Formatted: Underline, Highlight

Formatted: Underline, Highlight

Formatted: Underline, Highlight

277 **significant amounts of unburnt jet fuel.** Additionally, a strong positive linear correlation was observed between
 278 the AlkOA factor identified in this study and the decane factor from NIST webbook ($R=0.83$) (NIST Mass
 279 Spectrometry Data Center, 1990), as well as between the AlkOA factor determined here and the AlkOA factor
 280 reported by Smith et al. (2022) ($R=0.93$). The positive linear correlation among these three factors suggests they
 281 are indicative of similar primary pollutants derived from fuel vapours or incomplete combustion products
 282 associated with jet fuel. Results are consistent with previous findings of another study (Smith et al., 2022). **The**
 283 **third factor, More Oxidised Oxygenated Organic Aerosol (MO-OOA), is a type of secondary organic aerosol**
 284 **(SOA) that can form from various origins and processes, such as photochemical processing of aged SOA and the**
 285 **regional-scale transport of chemical reactions.** MO-OOA has a spectral fingerprint that consists of more oxidised
 286 ions (compared to LO-OOA and AlkOA), indicating a secondary aerosol fraction in the sample. **MO-OOA is**
 287 **characterized by its notably high relative intensities (>0.18) at m/z 29 and 44, which serve as markers for its**
 288 **identification.** Given that MO-OOA has the highest $f_{44/43}$ ratio among the three factors, it is expected to be the
 289 most oxygenated **(in terms of chemical content)** factor. Being more oxidised potentially makes MO-OOA less
 290 volatile than LO-OOA (Jimenez et al., 2009; Smith et al., 2022). **MO-OOA in this analysis indicates the formation**
 291 **of aged secondary organic aerosols with no significant diurnal variation (Fig. 5), often associated with air masses**
 292 **transported from polluted regions.** Other sources may have been included in one or both factor solutions,
 293 consequently, this does not rule out the possibility of their existence.

294 3.3 The temporal distribution of factors and correlation with trace gases



298 **Figure 5. Diurnal pattern of the solved factors from October 8, 2021 to October 23, 2021. Compared to LO-OOA and**
 299 **AlkOA; MO-OOA has the smallest variation in its diurnal pattern.**

302 Average hourly concentrations of the PMF determined factors were calculated to monitor the diurnal variation of
 303 the source contributions. The variation of the AlkOA concentration during the day mostly associated with aircraft
 304 emissions (Fig. 5). The concentration of AlkOA factor is relatively higher in the afternoon compared to the
 305 morning and midday. **The pattern of diurnal AlkOA closely resembles that of diurnal flight activities, suggesting**
 306 **that the surge in AlkOA levels beginning at noon is linked to primary particles released by aircraft. Further details**
 307 **on daily aircraft activities can be found in the supplementary material (Fig. S2).** This source has been previously
 308 reported as the main determinant of the air quality in the vicinity of the airport (Masiol and Harrison, 2014). **The**
 309 **LO-OOA factor likely represents fresh secondary organic aerosols (SOA), demonstrating high variability and**
 310 **sensitivity to ambient temperature fluctuations.** The concentration of LO-OOA is at its lowest when daytime
 311 temperatures peak. LO-OOA may contain urban contributions and potentially effected by background urban
 312 pollution from Madrid. The observed reduction in LO-OOA factor during the afternoon can be attributed to
 313 dilution effects resulting from the rise in boundary layer height, along with the potential evaporation of LO-OOA
 314 particles due to increased ambient temperatures. **This is supported by the variance in background particulate matter**
 315 **concentrations located south of the airport compared to those at the sampling point, approximately 6 km apart, as**
 316 **illustrated in Fig. S3. (Fig. S3) reveals that $PM_{2.5}$ levels at both locations experience significant increases during**
 317 **morning and evening rush hours, with the sampling point consistently showing higher concentrations than the**
 318 **background location. The diurnal pattern of the background location demonstrates a rapid decrease in $PM_{2.5}$ levels**
 319 **in the afternoon, unlike the measurements at the sampling point. Additionally, there is a noticeable lag of about**
 320 **an hour between the peak concentrations at the sampling point and those in the background, suggesting the**
 321 **influence of additional combustion sources of $PM_{2.5}$, notably aviation-related activities, particularly during periods**
 322 **of increased airport traffic.** Unlike other factors, MO-OOA shows no significant diurnal variation, indication the

323 formation of aged secondary organic aerosols, often a result of atmospheric transport (Zhang et al., 2007). At
 324 Madrid-Barajas Airport, AlkOA exhibited moderate correlations with *e*BC, NO_x, SO₂, and CO, as evidenced by
 325 the linear correlation coefficients listed in Table 1 (R=0.56, R =0.52, R =0.53, and R =0.52). In contrast, the
 326 correlation of these trace gases and both LO-OOA and MO-OOA is lower compared to AlkOA, with R values
 327 ranging from 0.2 to 0.5, as shown in (Table 1). The slightly higher correlation of AlkOA with BC, NO_x, SO₂ and
 328 CO (R > 0.5) relative to LO-OOA and MO-OOA can be attributed to AlkOA being a primary pollutant, emitted
 329 directly from the source. Conversely, LO-OOA and MO-OOA are believed to be secondary pollutants, formed
 330 through the processes of condensation and coagulation of primary pollutants. In this study, urban contributions
 331 are predominantly subject to this processing, as there is insufficient time for significant photochemical oxidation
 332 of aviation emissions in such close proximity to the source. Additionally, the diurnal trends of BC, NO_x, SO₂ and
 333 CO can be significantly affected by meteorological conditions (*e.g.*, wind speed, temperature) (Carslaw et al.,
 334 2006; Reyes et al., 2018). This influence accounts for their moderate correlation with AlkOA, with R values
 335 between 0.52 and 0.56, as detailed in Table 1. AlkOA and trace gases were normalised to facilitate comparison of
 336 their diurnal patterns, thereby enhancing understanding of their relative contributions and identifying trends
 337 among these pollutants. Normalising is accomplished by dividing the concentrations of the pollutants by their
 338 average value. Figure 6 shows diurnal patterns of AlkOA factor, *e*BC, NO_x, CO, and particle number
 339 concentration. The daily trend of *e*BC, NO_x and CO are mostly similar, with very pronounced increases in
 340 concentrations during the morning and evening rush hours. The average concentrations were 1.07 µg/m³, 22.7
 341 µg/m³ and 0.23 mg/m³ for *e*BC, NO_x and CO respectively (Table S1). AlkOA gradually increases during the
 342 morning, with multiple minor peaks observed in the morning hours. The average concentration of AlkOA is higher
 343 at night than during the day. This increase is potentially related to daily aircraft activities. AlkOA began to
 344 increase, reaching a maximum during the afternoon rush hour from 12:00-18:00. a second rapid increase occurred
 345 around 20:00, potentially caused by an increase in the number of flights at this time (Fig. S2). Early morning
 346 AlkOA concentrations are significantly lower compared to those of *e*BC, NO_x and CO. This difference could be
 347 attributed to reduced emissions resulting from decreased aircraft activities in early mornings (Fig. S2). The rise in
 348 trace gases and *e*BC observed in the early morning hours could originate from various airport operations. Such
 349 operations might encompass emissions from auxiliary power units, vehicle traffic, and the use of ground service
 350 equipment at the airport (Masiol and Harrison, 2014). The total number concentration exhibited a temporal pattern
 351 similar to that of AlkOA from 15:00–21:00. Likewise, the temporal profiles of AlkOA and trace gases were similar
 352 during the afternoon period (17:00-21:00). This similarity in temporal profiles suggests common source origins,
 353 which may be temporally associated with aircraft activity or the influence of background urban pollution.

Formatted: Underline, Highlight

Formatted: Underline, Highlight

Formatted: Underline, Highlight

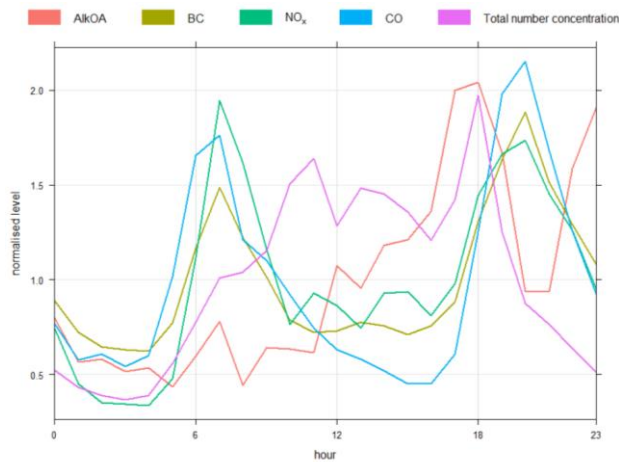
Formatted: Underline, Highlight

Formatted: Underline, Highlight

354 **Table 1 Results of linear regression analysis between obtained factors (LO-OOA, AlkOA, and MO-OOA) and**
 355 **external tracers.**
 356

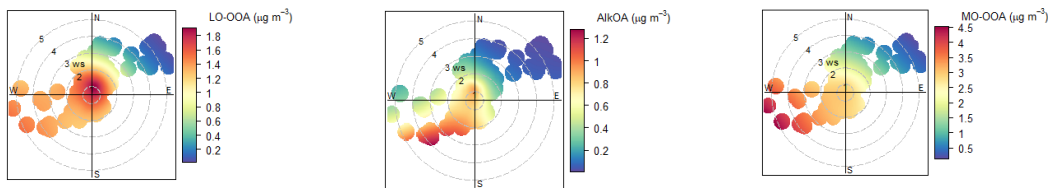
	<i>e</i> BC (µg/m ³)	NO _x (µg/m ³)	SO ₂ (µg/m ³)	CO (mg/m ³)	THC (mg/m ³)	PM2.5 (µg/m ³)	Tot No. conc (particles/cm ³)	CO ₂ (ppm)
LO-OOA	0.49	0.28	0.21	0.32	0.63	0.36	-0.08	0.24
AlkOA	0.56	0.52	0.53	0.52	0.35	0.66	0.4	0.35
MO-OOA	0.48	0.36	0.26	0.45	0.41	0.55	0.1	0.22

357
 358
 359
 360



361
362 **Figure 6. The diurnal cycle of AlkOA compared to eBC, NO_x, CO, and total number concentration. In this plot, the**
363 **concentrations are normalised with the objective of comparing the patterns of different pollutants using the same**
364 **scale.**

365
366 **3.4 Spatial analysis**
367



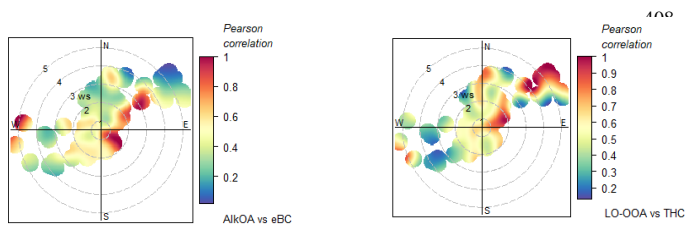
368
369 **Figure 7. Bivariate polar plots for LO-OOA, AlkOA, and MO-OOA ($\mu\text{g}/\text{m}^3$). The highest concentrations were**
370 **measured when the winds were originated from the west and southwest. Runways 18R/36L and 14R/32L located at**
371 **western and eastern sides of the measurement station and the hanger zone with terminals T1, T2, T3, T4, and TS4**
372 **are located at the south and southwest of the measurement site (Fig. 1).**

373
374 Varying sources can be discriminated by means of bivariate polar plots techniques (Carslaw and Ropkins, 2012).
375 Figure 7 illustrates the impact of airport activities on the average concentrations of factors (LO-OOA, AlkOA and
376 MO-OOA) as determined by PMF. The highest concentrations of AlkOA and MO-OOA were observed at low to
377 moderate wind speeds (3–5 m/s) coming from the west and southwest ($R = -0.35$ and $R = -0.42$, respectively), near
378 the terminal buildings (T1, T2, T3, T4 and TS4), two of the runways (14R/32L and 18R/36L), and a nearby hanger
379 zone. The most significant contributions of LO-OOA occur at wind speeds below 2 m/s, with a correlation of $R =$
380 -0.45 . At such low wind speeds (< 2 m/s), LO-OOA and MO-OOA are more likely to be mixed and influenced
381 by a nearby source (Crilley et al., 2015; Helin et al., 2018). By contrast, the minimum significant contribution
382 from all factors was observed when the winds originated from the northeast of the airport, accompanied by
383 relatively higher wind speeds (above 4 m/s). Thus, based on the polar plots shown in Fig. 7, emissions from the
384 terminal buildings and hanger zone located at the southwest of the measurement station are the major sources of
385 total organic particle concentrations at the measurement station. The average contributions of LO-OOA, AlkOA,
386 and MO-OOA were 1.63, 0.63, and 2.35 $\mu\text{g}/\text{m}^3$, respectively (Table S1). During the AVIATOR campaign in
387 October 2021, LO-OOA and MO-OOA constituted more than 80% of the total organic mass. **Based on the strength**
388 **of the relationship outlined in Table 1 between derived factors and external tracers, the linear correlations (Pearson**
389 **correlation) between (i) AlkOA with eBC and (ii) LO-OOA with THC were measured under varying wind speed**
390 **and directions, as illustrated in (Fig. 8).** The relative contributions of the AlkOA and LO-OOA were higher with

Formatted: Underline, Highlight

391 winds originating from southwest of the airport, compared to when winds carried air parcels to the sampling point
 392 from the northeast, as discussed. However, the correlation coefficient for these factors varies significantly, ranging
 393 from 0.2 to 0.9, for all samples collected from various directions within the airport perimeter. For instance, AlkOA
 394 exhibits a strong linear correlation with eBC (Pearson coefficient higher than 0.9) when winds originate from the
 395 west, east, or northeast, as illustrated in Fig. 8. This correlation is attributed to the impact of runways 18L/36R
 396 and 18R/36L, which are situated to the east and west of the measurement site, respectively, as depicted in Fig. 1,
 397 where 90% of aircraft take-offs occur. Both AlkOA and eBC are related to jet fuel emissions, as they are directly
 398 emitted by aircraft engines as a result of fuel combustion. eBC emissions are a function of engine power settings,
 399 reaching their maximum at full thrust during take-off (Kinsey et al., 2011; Hu et al., 2009). Furthermore, a
 400 significant linear correlation was measured between LO-OOA and THC when dominant winds were north
 401 easterlies (the air parcels move from runways 18L/36R to the sampling station). THC emissions at airports
 402 primarily dependent on the jet engine thrust setting (Anderson et al., 2006; Onasch et al., 2009). When engines
 403 operate at low thrust settings (e.g., during landing, taxiing, idling), combustion is less efficient, leading to the
 404 emission of higher amounts of hydrocarbons. The association between LO-OOA and THC in certain areas of the
 405 airport can be interpreted as indicative of fresh emissions from aircraft in service.

- Formatted: Underline, Highlight
- Formatted: Underline, Highlight
- Formatted: Underline, Highlight
- Formatted: Underline, Highlight
- Formatted: Underline, Highlight
- Formatted: Underline, Highlight



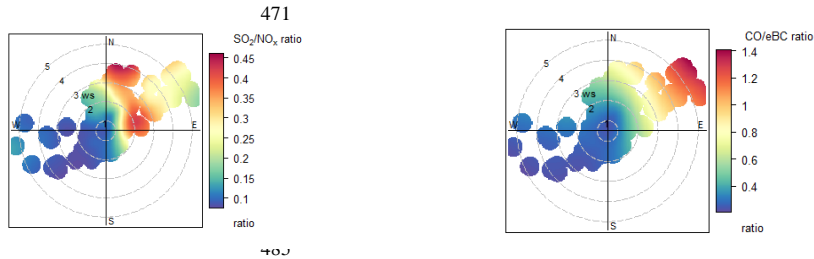
421
 422 **Figure 8. A Pearson correlation analysis using bivariate polar plots (above) shows a significant positive linear**
 423 **correlation between AlkOA with eBC and LO-OOA with THC mass concentrations when prevailing winds were**
 424 **northeast. (The location of runways 18L/36R).**
 425

426 NO_x emitted by aircraft can potentially affect air quality up to 2.6 km away from the airport (Carslaw et al., 2006).
 427 However, accurately determining the airport's contribution to local NO_x concentrations presents challenges due
 428 to other predominantly mobile sources of NO_x in urban areas. In this study, the potential contribution of road
 429 traffic surrounding the airport, particularly from the motorways located to the south and southwest, originates
 430 from the same direction as runway 14R/32L and all the terminals. Therefore, NO_x contributions were higher from
 431 the south and southwest of the airport (including local on-road NO_x) compared to the those from the northeast.
 432 The lowest NO_x concentrations were measured under moderate wind speed conditions (above 4 m/s), as shown in
 433 Fig. S1. This is possibly due to atmospheric mixing and plume dilution caused by advection (Carslaw et al., 2006),
 434 given that ground-level source emissions are inversely proportional to wind speed. During this campaign, the
 435 AENA (REDAIR) station located at the airport provided measurements of sulphur dioxide (SO₂) and carbon
 436 monoxide (CO) (Fig. S1). Aviation activities have previously been reported as a significant source of gaseous and
 437 vapour-phase pollutants, such as SO₂, CO and NO_x (Masiol and Harrison, 2014). In the same vein, mobile sources,
 438 such as vehicle exhaust, generally contribute to the increase in CO and NO_x levels, as motor vehicle emissions
 439 are the dominant sources of CO and NO_x emissions in urban areas (Yu et al., 2004). Given that Barajas airport is
 440 situated near Madrid and significantly influenced by external sources, particularly traffic on the southwest side of
 441 the airport, it experiences considerable environmental impact. Therefore, the ratios of SO₂/NO_x and CO/eBC were
 442 used in this analysis as indicators of the relative emission strengths associated with aircraft movements. The
 443 SO₂/NO_x ratio would increase in the case of aviation emissions compared to traffic emissions, since NO_x emissions
 444 from aircraft are difficult to distinguish due to the major influence of other sources (Yu et al., 2004; Carslaw et
 445 al., 2006). Consequently, in situations where there are substantial levels of NO_x emissions, the SO₂/NO_x ratio will
 446 be low due to the impact of on-road vehicles emissions. This enables the identification of aircraft's relative
 447 contribution at the airport, as shown in Fig.9. The analysis of the SO₂/NO_x and CO/eBC concentration ratios at
 448 Madrid-Barajas Airport in October 2021 varies based on wind direction and speed. The bivariate polar plots shown
 449 in Fig. 9 indicate higher SO₂/NO_x and CO/eBC ratios were measured when dominant winds originating from the
 450 northeast of the airport, where there was minimal or no contribution from road traffic. The higher SO₂/NO_x and
 451 CO/eBC ratios suggest the potential impact of aircraft taxiing and taking off on local ambient SO₂ and CO
 452 concentrations, particularly when winds originate from northeast, where the 18L/36R runways are located. SO₂

- Formatted: Underline, Highlight
- Formatted: Underline, Highlight
- Formatted: Underline, Highlight
- Formatted: Underline, Highlight
- Formatted: Underline, Highlight
- Formatted: Underline, Highlight
- Formatted: Underline, Highlight
- Formatted: Underline, Highlight
- Formatted: Underline, Highlight
- Formatted: Underline, Highlight
- Formatted: Underline, Highlight

emissions are primarily associated with the sulphur content of the fuel and emissions from aircraft activities at the airport, such as approach, taxi-idle and climb. As a result, SO₂ plays a significant role in tracing aircraft emissions at a local scale (Yang et al., 2018). Black carbon (eBC) and carbon monoxide (CO) are primarily produced by incomplete or inefficient combustion. Around the airport perimeter, aircraft are a significant contributor to CO emissions. Therefore, it's possible for aircraft engines to emit more CO compared to emissions from road traffic, due to the duration spent at the airport in taxiing /idling mode (Yu et al., 2004; Zhu et al., 2011). The CO/eBC ratio significantly varies with the source (Bond et al., 2004), indicating the presence of different emission sources in the vicinity of the airport, as previously reported. The highest levels of CO from aircraft are emitted at low engine power settings, such as during taxiing and idling. This significantly impacts air quality within the airport perimeter, as idle and taxi phases constitute the majority of the time an aircraft spends at the airport (Stettler et al., 2011; Yunos et al., 2017). Higher CO/eBC ratio in air parcels originating from the northeast can also be attributed to aircraft activity on runways 18L/36R, which is located northeast of the measurement station. Conversely, SO₂/NO_x and CO/eBC ratios were lower (ranging from 0 to 0.4) when winds originated from the southwest, due to significant sources of NO_x and eBC in this direction, such as nearby road traffic. Based on the polar plots shown in Fig. 9, an aircraft SO₂ and CO signal is identified to the east and northeast, distinct from the wind-dependant NO_x pattern. Further details regarding the daily variation of meteorological parameters and trace gases during the sampling period are available in the supplementary material (Fig. S1).

470



486 **Figure 9. Bivariate polar plots of SO₂/NO_x and CO/eBC ratios at the airport. The angular contributions of SO₂ and**
 488 **CO is different compared to the PMF determined factors. The plots indicates that the flight activities at the east and**
 489 **northeast where the 18L/36R runway is located are the source of increase in SO₂ and CO.**

490 **4. Conclusion**

492 This study identified the impact of an international airport on the local air quality. As part of the AVIATOR
 493 campaign, several measurements were conducted at the Madrid-Barajas Airport, in October 2021 for monitoring
 494 the chemical composition of sub-micron particles and ambient trace gas concentrations near runway. Assessing
 495 the impact of Madrid-Barajas Airport emissions on local air quality is challenging because of the complex nature
 496 of airport emissions and the strong influence from urban emissions. The proximity of the airport to urban areas,
 497 major highways, roads, and terminal buildings (T1, T2, T3, T4 and TS4) further complicates the task, making it
 498 difficult to clearly identify the specific contributions of aircraft emissions. However, aircraft emissions are
 499 characterized by high levels of unburned hydrocarbons, SO₂, CO and particulate black carbon (eBC) which are
 500 more concentrated around the airport facilities and runways. Therefore, looking at elevated levels of these markers
 501 might indicate a stronger influence from aviation-related activities, especially during times of high airport traffic.
 502 Total non-refractory particles were dominated by organics (more than 72% of the total). Sulphate particles were
 503 the second most abundant chemical species and accounted for about 13% of the total aerosol. Based on AMS data
 504 (Ratio of *m/z* 85:71), no significant oil fraction in the organic particulate matter (PM) samples were measured.
 505 This could indicate the absence of oil in sub-micron particle size range or due to the method used in this study
 506 (AMS) is not able to identify lubricant oil in PM. Thus, further measurements with improved measurement
 507 technique may be required to identify oil fraction in sub-micron organic aerosol. Trace gases were also monitored
 508 along with the particle monitoring tools. Average ambient concentrations of eBC, NO_x, SO₂, PM_{2.5}, PM₁₀ at the
 509 airport during October 2021 were 1.07, 22.7, 4.10, 9.35, and 16.43 (µg/m³), respectively. NO_x contribution at the
 510 sampling point was highest when the winds originating from south and southeast of the airport. There are two
 511 motorways with road traffic are located at the same direction as well as terminal buildings and southern runways.
 512 Therefore, NO_x concentrations were more likely determined by on-road traffic compared to the aircraft activity at
 513 the sampling point. Sources of organic aerosols (as the most abundant non-refractory aerosol group) were
 514 identified using Positive Matrix Factorisation (PMF) analysis. PMF was able to discriminate three main significant

- Formatted: Underline, Highlight
- Formatted: Underline, Highlight
- Formatted: Underline, Highlight
- Formatted: Underline, Highlight
- Formatted: Underline, Highlight
- Formatted: Underline, Highlight
- Formatted: Underline, Highlight
- Formatted: Underline, Highlight

Formatted: Underline, Highlight

516 sources: Less Oxidised Oxygenated Organic Aerosol (LO-OOA), Alkane Organic Aerosol (AlkOA), and More
517 Oxidised Oxygenated Organic Aerosol (MO OOA). The sum of LO-OOA and MO OOA fractions accounting for
518 more than 80% of the total organic mass throughout the campaign, LO-OOA had the highest relative intensity
519 (RI) at m/z 43 (which is characteristic of LO-OOA), MO-OOA had a high RI at m/z 28 and 44 these indicate a
520 potential secondary aerosol fraction. Third factor, AlkOA, had high RIs at m/z 43, 57 and 85 (attributed to decane
521 previously) which is related to jet fuel vapour (Smith et al., 2022). Bivariate polar plots were used to angular PMF
522 determined factor and ambient trace gas distributions based on wind speed and wind direction at the airport. It has
523 been found that, the PMF determined factors had highest relative contributions when the winds originating from
524 the west and southwest of the airport where runways 14R/32L and 18R/36L, as well as terminals T1, T2, T3, T4
525 and TS4, are located. The SO_2/NO_x and CO/eBC ratio have been shown to represent a useful tool for assessing
526 relative emission strength associated with aircraft movements. Take-off activities at the northeast of the
527 measurement station were identified as a potential local source of SO_2 and CO in Barajas-Madrid. Angular
528 correlation analysis based on wind direction and speed indicated that eBC and THC emissions are potentially
529 determined by aircraft take off activities at 18L/36R runway located along the east and northeast of the sampling
530 point where more than 50% of the take-off activity took place in the sampling period.

Formatted: Underline, Highlight

Formatted: Underline, Highlight

Formatted: Underline

531 There are two previously reported significant ways to reduce aviation emissions at airports, improving efficiency
532 of the processes emitting air pollutants such as electrification of airport taxiway operations (Salihu et al., 2021),
533 and switching to sustainable alternative fuels where applicable. Improved ground activities at airports such as
534 electric aircraft towing system can potentially lead up to 82 % reduction in CO_2 emissions (van Baaren, 2019),
535 while switching to SAF alone reduce Landing-takeoff cycle (LTO) emissions up to 70 % compared to fossil fuel
536 (Schripp et al., 2022). Further, SAF use for auxiliary power units (APU) also potentially reduce NO_x and CO_2
537 emissions by at least 5%. Therefore, improving energy efficiency of ground activities at airports and using SAF
538 are recommended for policymakers to improve the overall air quality at airports.

539 *Author contributions.* **Saleh Alzahrani, Doğuşhan Kılıç, Michael Flynn, Paul I. Williams and James Allan**
540 designed the project; **Saleh Alzahrani, Doğuşhan Kılıç, Michael Flynn and Paul I. Williams** performed the
541 fieldwork; **Saleh Alzahrani** performed the data analysis, and wrote – original draft of the article; **Doğuşhan**
542 **Kılıç** reviewed and edited the article; **Paul I. Williams and James Allan** supervised, reviewed and edited the
543 article.
544

545 *Competing interests.* At least one of the (co-) authors is a member of the editorial board of Atmospheric
546 Chemistry and Physics.
547

548 Acknowledgments

549 This project has received funding from the European Union's Horizon 2020 research and innovation programme
550 under Grant Agreement No 814801.
551

552 References

- 553 Air transport statistics: europa.eu, 2022.
554
555 Amato, F., Moreno, T., Pandolfi, M., Querol, X., Alastuey, A., Delgado, A., Pedrero, M. and Cots, N.:
556 Concentrations, sources and geochemistry of airborne particulate matter at a major European airport. *Journal of*
557 *Environmental Monitoring*, 12(4), pp.854-862, <https://doi.org/10.1039/B925439K>, 2010.
558
559 Anderson, B.E., Beyersdorf, A.J., Hudgins, C.H., Plant, J.V., Thornhill, K.L., Winstead, E.L., Ziemba, L.D.,
560 Howard, R., Corporan, E., Miake-Lye, R.C. and Herndon, S.C.: Alternative aviation fuel experiment
561 (AAFEX) (No. NASA/TM-2011-217059), 2011.
562
563 Anderson, B.E., Chen, G. and Blake, D.R.: Hydrocarbon emissions from a modern commercial
564 airliner. *Atmospheric Environment*, 40(19), pp.3601-3612, <https://doi.org/10.1016/j.atmosenv.2005.09.072>,
565 2006.
566
567 Bond, T.C., Streets, D.G., Yarber, K.F., Nelson, S.M., Woo, J.H. and Klimont, Z.: A technology-based global
568 inventory of black and organic carbon emissions from combustion. *Journal of Geophysical Research:*
569 *Atmospheres*, 109(D14), <https://doi.org/10.1029/2003JD003697>, 2004.
570
571
572
573

574 Boldo, E., Medina, S., Le Tertre, A., Hurley, F., Mücke, H.G., Ballester, F., Aguilera, I. and Daniel Eilstein on
575 behalf of the Apehis group.: Apehis: Health impact assessment of long-term exposure to PM 2.5 in 23 European
576 cities. *European journal of epidemiology*, 21, pp.449-458, <https://doi.org/10.1007/s10654-006-9014-0>, 2006.
577

578 Canagaratna, M.R., Jayne, J.T., Jimenez, J.L., Allan, J.D., Alfarra, M.R., Zhang, Q., Onasch, T.B., Drewnick,
579 F., Coe, H., Middlebrook, A. and Delia, A.: Chemical and microphysical characterization of ambient aerosols
580 with the aerodyne aerosol mass spectrometer. *Mass spectrometry reviews*, 26(2), pp.185-222,
581 <https://doi.org/10.1002/mas.20115>, 2007.
582

583 Canonaco, F., Crippa, M., Slowik, J.G., Baltensperger, U. and Prévôt, A.S.: SoFi, an IGOR-based interface for
584 the efficient use of the generalized multilinear engine (ME-2) for the source apportionment: ME-2 application to
585 aerosol mass spectrometer data. *Atmospheric Measurement Techniques*, 6(12), pp.3649-3661,
586 <https://doi.org/10.5194/amt-6-3649-2013>, 2013.
587

588 Carslaw, D.C., Beevers, S.D., Ropkins, K. and Bell, M.C.: Detecting and quantifying aircraft and other on-
589 airport contributions to ambient nitrogen oxides in the vicinity of a large international airport. *Atmospheric
590 Environment*, 40(28), pp.5424-5434, <https://doi.org/10.1016/j.atmosenv.2006.04.062>, 2006.
591

592 Carslaw, D.C. and Ropkins, K.: Openair—an R package for air quality data analysis. *Environmental Modelling
593 & Software*, 27, pp.52-61, <https://doi.org/10.1016/j.envsoft.2011.09.008>, 2012.
594

595 Crilley, L.R., Bloss, W.J., Yin, J., Beddows, D.C., Harrison, R.M., Allan, J.D., Young, D.E., Flynn, M.,
596 Williams, P., Zotter, P. and Prévôt, A.S.: Sources and contributions of wood smoke during winter in London:
597 assessing local and regional influences. *Atmospheric chemistry and physics*, 15(6), pp.3149-3171,
598 <https://doi.org/10.5194/acp-15-3149-2015>, 2015.
599

600 Environmental protection. Annex 16 to the Convention on International Civil Aviation. Volume II aircraft
601 engine emissions. I.C.A.O., 2016.
602

603 Fushimi, A., Saitoh, K., Fujitani, Y. and Takegawa, N.: Identification of jet lubrication oil as a major component
604 of aircraft exhaust nanoparticles. *Atmospheric Chemistry and Physics*, 19(9), pp.6389-6399, 2019.
605

606 He, R.W., Shirmohammadi, F., Gerlofs-Nijland, M.E., Sioutas, C. and Cassee, F.R.: Pro-inflammatory
607 responses to PM_{0.25} from airport and urban traffic emissions. *Science of the total environment*, 640, pp.997-
608 1003, <https://doi.org/10.1016/j.scitotenv.2018.05.382>, 2018.
609

610 Herndon, S.C., Jayne, J.T., Lobo, P., Onasch, T.B., Fleming, G., Hagen, D.E., Whitefield, P.D. and Miale-Lye,
611 R.C.: Commercial aircraft engine emissions characterization of in-use aircraft at Hartsfield-Jackson Atlanta
612 International Airport. *Environmental science & technology*, 42(6), pp.1877-1883,
613 <https://doi.org/10.1021/es072029+>, 2008.
614

615 Helin, A., Niemi, J.V., Virkkula, A., Pirjola, L., Teinilä, K., Backman, J., Aurela, M., Saarikoski, S., Rönkkö,
616 T., Asmi, E. and Timonen, H.: Characteristics and source apportionment of black carbon in the Helsinki
617 metropolitan area, Finland. *Atmospheric Environment*, 190, pp.87-98,
618 <https://doi.org/10.1016/j.atmosenv.2018.07.022>, 2018.
619

620 Hu, S., Fruin, S., Kozawa, K., Mara, S., Winer, A.M. and Paulson, S.E.: Aircraft emission impacts in a
621 neighborhood adjacent to a general aviation airport in Southern California. *Environmental science &
622 technology*, 43(21), pp.8039-8045, <https://doi.org/10.1021/es900975f>, 2009.
623

624 Hudda, N. and Fruin, S.A.: International airport impacts to air quality: size and related properties of large
625 increases in ultrafine particle number concentrations. *Environmental science & technology*, 50(7), pp.3362-
626 3370, <https://doi.org/10.1021/acs.est.5b05313>, 2016.
627

628 Hudda, N., Gould, T., Hartin, K., Larson, T.V. and Fruin, S.A.: Emissions from an international airport increase
629 particle number concentrations 4-fold at 10 km downwind. *Environmental science & technology*, 48(12),
630 pp.6628-6635, <https://doi.org/10.1021/es5001566>, 2014.
631

632 Hudda, N., Simon, M.C., Zamore, W., Brugge, D. and Durant, J.L.: Aviation emissions impact ambient ultrafine
633 particle concentrations in the greater Boston area. *Environmental science & technology*, 50(16), pp.8514-8521,
634 <https://doi.org/10.1021/acs.est.6b01815>, 2016.

635
636 Jimenez, J.L., Canagaratna, M.R., Donahue, N.M., Prevot, A.S.H., Zhang, Q., Kroll, J.H., DeCarlo, P.F., Allan,
637 J.D., Coe, H., Ng, N.L. and Aiken, A.C.: Evolution of organic aerosols in the atmosphere. *Science*, 326(5959),
638 pp.1525-1529, <https://doi.org/10.1126/science.118035>, 2009.

639
640 Jonsdottir, H.R., Delaval, M., Leni, Z., Keller, A., Brem, B.T., Siegerist, F., Schönenberger, D., Durdina, L.,
641 Elser, M., Burtscher, H. and Liati, A.: Non-volatile particle emissions from aircraft turbine engines at ground-
642 idle induce oxidative stress in bronchial cells. *Communications biology*, 2(1), p.90,
643 <https://doi.org/10.1038/s42003-019-0332-7>, 2019.

644
645 Kinsey, J.S.: Characterization of emissions from commercial aircraft engines during the Aircraft Particle
646 Emissions eXperiment (APEX) 1 to 3. Office of Research and Development, US Environmental Protection
647 Agency, 2009.

648
649 Kinsey, J.S., Dong, Y., Williams, D.C. and Logan, R.: Physical characterization of the fine particle emissions
650 from commercial aircraft engines during the Aircraft Particle Emissions eXperiment (APEX) 1–3. *Atmospheric
651 Environment*, 44(17), pp.2147-2156, <https://doi.org/10.1016/j.atmosenv.2010.02.010>, 2010.

652
653 Kinsey, J.S., Hays, M.D., Dong, Y., Williams, D.C. and Logan, R.: Chemical characterization of the fine
654 particle emissions from commercial aircraft engines during the Aircraft Particle Emissions eXperiment (APEX)
655 1 to 3. *Environmental science & technology*, 45(8), pp.3415-3421, <https://doi.org/10.1021/es103880d>, 2011.

656
657 Lee, D.S., Pitari, G., Grewe, V., Gierens, K., Penner, J.E., Petzold, A., Prather, M.J., Schumann, U., Bais, A.,
658 Bernsten, T. and Iachetti, D.: Transport impacts on atmosphere and climate: Aviation. *Atmospheric
659 environment*, 44(37), pp.4678-4734, <https://doi.org/10.1016/j.atmosenv.2009.06.005>, 2010.

660
661 Li, N., Hao, M., Phalen, R.F., Hinds, W.C. and Nel, A.E.: Particulate air pollutants and asthma: a paradigm for
662 the role of oxidative stress in PM-induced adverse health effects. *Clinical immunology*, 109(3), pp.250-265,
663 <https://doi.org/10.1016/j.clim.2003.08.006>, 2003.

664
665 Liu, G., Yan, B. and Chen, G.: Technical review on jet fuel production. *Renewable and Sustainable Energy
Reviews*, 25, pp.59-70, 2013.

666
667 Masiol, M. and Harrison, R.M.: Aircraft engine exhaust emissions and other airport-related contributions to
668 ambient air pollution: A review. *Atmospheric Environment*, 95, pp.409-455,
669 <https://doi.org/10.1016/j.atmosenv.2014.05.070>, 2014.

670
671 Mazaheri, M., Johnson, G.R. and Morawska, L.: An inventory of particle and gaseous emissions from large
672 aircraft thrust engine operations at an airport. *Atmospheric Environment*, 45(20), pp.3500-3507,
673 <https://doi.org/10.1016/j.atmosenv.2010.12.012>, 2011.

674
675 NIST Mass Spectrometry Data Center. Decane, US secretary of commerce.
676 <https://webbook.nist.gov/cgi/cbook.cgi?ID=C124185&Mask=200#Mass-Spec>, 1990.

677
678 Onasch, T.B., Jayne, J.T., Herndon, S., Worsnop, D.R., Miake-Lye, R.C., Mortimer, I.P. and Anderson, B.E.:
679 Chemical properties of aircraft engine particulate exhaust emissions. *Journal of Propulsion and Power*, 25(5),
680 pp.1121-1137, <https://doi.org/10.2514/1.36371>, 2009.

681
682 Paatero, P.: The multilinear engine—a table-driven, least squares program for solving multilinear problems,
683 including the n-way parallel factor analysis model. *Journal of Computational and Graphical Statistics*, 8(4),
684 pp.854-888, <https://doi.org/10.1080/10618600.1999.10474853>, 1999.

685
686 Paatero, P. and Tapper, U.: Positive matrix factorization: A non-negative factor model with optimal utilization
687 of error estimates of data values. *Environmetrics*, 5(2), pp.111-126, <https://doi.org/10.1002/env.3170050203>,
688 1994.

687
688 Petzold, A. and Schönlinner, M.: Multi-angle absorption photometry—a new method for the measurement of
689 aerosol light absorption and atmospheric black carbon. *Journal of Aerosol Science*, 35(4), pp.421-441,
690 <https://doi.org/10.1016/j.jaerosci.2003.09.005>, 2004.
691

692 Pope III, C.A. and Dockery, D.W.: Health effects of fine particulate air pollution: lines that connect. *Journal of*
693 *the air & waste management association*, 56(6), pp.709-742, <https://doi.org/10.1080/10473289.2006.10464485>,
694 2006.

695 Reyes-Villegas, E., Green, D.C., Priestman, M., Canonaco, F., Coe, H., Prévôt, A.S. and Allan, J.D.: Organic
696 aerosol source apportionment in London 2013 with ME-2: exploring the solution space with annual and seasonal
697 analysis. *Atmospheric Chemistry and Physics*, 16(24), pp.15545-15559, [https://doi.org/10.5194/acp-16-15545-](https://doi.org/10.5194/acp-16-15545-2016)
698 2016, 2016.
699

700 Reyes-Villegas, E., Priestley, M., Ting, Y.C., Haslett, S., Bannan, T., Le Breton, M., Williams, P.I., Bacak, A.,
701 Flynn, M.J., Coe, H. and Percival, C.: Simultaneous aerosol mass spectrometry and chemical ionisation mass
702 spectrometry measurements during a biomass burning event in the UK: insights into nitrate
703 chemistry. *Atmospheric Chemistry and Physics*, 18(6), pp.4093-4111, [https://doi.org/10.5194/acp-18-4093-](https://doi.org/10.5194/acp-18-4093-2018)
704 2018, 2018.
705

706 Rissman, J., Arunachalam, S., Woody, M., West, J.J., BenDor, T. and Binkowski, F.S.: A plume-in-grid
707 approach to characterize air quality impacts of aircraft emissions at the Hartsfield–Jackson Atlanta International
708 Airport. *Atmospheric Chemistry and Physics*, 13(18), pp.9285-9302, <https://doi.org/10.5194/acp-13-9285-2013>,
709 2013.
710

711 Salihi, A.L., Lloyd, S.M. and Akgunduz, A.: Electrification of airport taxiway operations: A simulation
712 framework for analyzing congestion and cost. *Transportation Research Part D: Transport and Environment*, 97,
713 p.102962, <https://doi.org/10.1016/j.trd.2021.102962>, 2021.
714

715 Schripp, T., Anderson, B.E., Bauder, U., Rauch, B., Corbin, J.C., Smallwood, G.J., Lobo, P., Crosbie, E.C.,
716 Shook, M.A., Miake-Lye, R.C. and Yu, Z.: Aircraft engine particulate matter emissions from sustainable
717 aviation fuels: Results from ground-based measurements during the NASA/DLR campaign ECLIF2/ND-
718 MAX. *Fuel*, 325, p.124764, <https://doi.org/10.1016/j.fuel.2022.124764>, 2022.
719

720 Schwarze, P.E., Øvreivik, J., Låg, M., Refsnes, M., Nafstad, P., Hetland, R.B. and Dybing, E.: Particulate matter
721 properties and health effects: consistency of epidemiological and toxicological studies. *Human & experimental*
722 *toxicology*, 25(10), pp.559-579, <https://doi.org/10.1177/096032706072520>, 2006.
723

724 Smith, L.D., Allan, J., Coe, H., Reyes-Villegas, E., Johnson, M.P., Crayford, A., Durand, E. and Williams, P.I.:
725 Examining chemical composition of gas turbine-emitted organic aerosol using positive matrix factorisation
726 (PMF). *Journal of Aerosol Science*, 159, p.105869, <https://doi.org/10.1016/j.jaerosci.2021.105869>, 2022.
727

728 Stettler, M.E.J., Eastham, S. and Barrett, S.R.H.: Air quality and public health impacts of UK airports. Part I:
729 Emissions. *Atmospheric environment*, 45(31), pp.5415-5424, <https://doi.org/10.1016/j.atmosenv.2011.07.012>,
730 2011.
731

732 Timko, M.T., Albo, S.E., Onasch, T.B., Fortner, E.C., Yu, Z., Miake-Lye, R.C., Canagaratna, M.R., Ng, N.L.
733 and Worsnop, D.R.: Composition and sources of the organic particle emissions from aircraft engines. *Aerosol*
734 *Science and Technology*, 48(1), pp.61-73, <https://doi.org/10.1080/02786826.2013.857758>, 2014.
735

736 Timko, M.T., Onasch, T.B., Northway, M.J., Jayne, J.T., Canagaratna, M.R., Herndon, S.C., Wood, E.C.,
737 Miake-Lye, R.C. and Knighton, W.B.: Gas turbine engine emissions—Part II: chemical properties of particulate
738 matter. <https://doi.org/10.1115/1.4000132>, 2010.
739

740 Ulbrich, I.M., Canagaratna, M.R., Zhang, Q., Worsnop, D.R. and Jimenez, J.L.: Interpretation of organic
741 components from Positive Matrix Factorization of aerosol mass spectrometric data. *Atmospheric Chemistry and*
742 *Physics*, 9(9), pp.2891-2918, <https://doi.org/10.5194/acp-9-2891-2009>, 2009.
743

744 Ungeheuer, F., Caudillo, L., Ditas, F., Simon, M., van Pinxteren, D., Kılıç, D., Rose, D., Jacobi, S., Kürten, A.,
745 Curtius, J. and Vogel, A.L.: Nucleation of jet engine oil vapours is a large source of aviation-related ultrafine
746 particles. *Communications Earth & Environment*, 3(1), p.319, <https://doi.org/10.1038/s43247-022-00653-w>,
747 2022.
748
749 van Baaren, E.: The feasibility of a fully electric aircraft towing system. 2019.
750
751 Westerdahl, D., Fruin, S.A., Fine, P.L. and Stoutas, C.: The Los Angeles International Airport as a source of
752 ultrafine particles and other pollutants to nearby communities. *Atmospheric Environment*, 42(13), pp.3143-
753 3155, <https://doi.org/10.1016/j.atmosenv.2007.09.006>, 2008.
754
755 Yang, X., Cheng, S., Lang, J., Xu, R. and Lv, Z.: Characterization of aircraft emissions and air quality impacts
756 of an international airport. *Journal of environmental sciences*, 72, pp.198-207,
757 <https://doi.org/10.1016/j.jes.2018.01.007>, 2018.
758
759 Yim, S.H., Stettler, M.E. and Barrett, S.R.: Air quality and public health impacts of UK airports. Part II: Impacts
760 and policy assessment. *Atmospheric environment*, 67, pp.184-192,
761 <https://doi.org/10.1016/j.atmosenv.2012.10.017>, 2013.
762
763 Yu, K.N., Cheung, Y.P., Cheung, T. and Henry, R.C.: Identifying the impact of large urban airports on local air
764 quality by nonparametric regression. *Atmospheric Environment*, 38(27), pp.4501-4507,
765 <https://doi.org/10.1016/j.atmosenv.2004.05.034>, 2004.
766
767 Yu, Z., Herndon, S.C., Ziemba, L.D., Timko, M.T., Liscinsky, D.S., Anderson, B.E. and Miake-Lye, R.C.:
768 Identification of lubrication oil in the particulate matter emissions from engine exhaust of in-service commercial
769 aircraft. *Environmental science & technology*, 46(17), pp.9630-9637, <https://doi.org/10.1021/es301692t>, 2012.
770
771 Yu, Z., Liscinsky, D.S., Winstead, E.L., True, B.S., Timko, M.T., Bhargava, A., Herndon, S.C., Miake-Lye,
772 R.C. and Anderson, B.E.: Characterization of lubrication oil emissions from aircraft engines. *Environmental*
773 *science & technology*, 44(24), pp.9530-9534, <https://doi.org/10.1021/es102145z>, 2010.
774
775 Yu, Z., Timko, M.T., Herndon, S.C., Richard, C., Beyersdorf, A.J., Ziemba, L.D., Winstead, E.L. and Anderson,
776 B.E.: Mode-specific, semi-volatile chemical composition of particulate matter emissions from a commercial gas
777 turbine aircraft engine. *Atmospheric Environment*, 218, p.116974,
778 <https://doi.org/10.1016/j.atmosenv.2019.116974>, 2019.
779
780 Yunos, S.N.M.M., Ghafir, M.F.A. and Wahab, A.A.: April. Aircraft LTO emissions regulations and
781 implementations at European airports. In *AIP Conference Proceedings* (Vol. 1831, No. 1),
782 <https://doi.org/10.1063/1.4981147>, 2017.
783
784 Zhang, Q., Jimenez, J.L., Canagaratna, M.R., Allan, J.D., Coe, H., Ulbrich, I., Alfarra, M.R., Takami, A.,
785 Middlebrook, A.M., Sun, Y.L. and Dzepina, K.: Ubiquity and dominance of oxygenated species in organic
786 aerosols in anthropogenically-influenced Northern Hemisphere midlatitudes. *Geophysical research*
787 *letters*, 34(13), <https://doi.org/10.1029/2007GL029979>, 2007.
788
789 Zhu, Y., Fanning, E., Yu, R.C., Zhang, Q. and Froines, J.R.: Aircraft emissions and local air quality impacts
790 from takeoff activities at a large International Airport. *Atmospheric Environment*, 45(36), pp.6526-6533,
791 <https://doi.org/10.1016/j.atmosenv.2011.08.062>, 2011.
792
793
794
795
796
797